

Visible light induced hydrogen evolution over the heterosystem $\text{Bi}_2\text{S}_3/\text{TiO}_2$

R. Brahimi, Y. Bessekhoud, A. Bouguelia, M. Trari*

Laboratoire de Stockage et de Valorisation des Energies Renouvelables, Faculté de Chimie (USTHB), BP 32, El Alia 16111 Algiers, Algeria

Available online 31 January 2007

Abstract

A new photochemical heterosystem $\text{Bi}_2\text{S}_3/\text{TiO}_2$ immersed in solutions of X^{2-} ($=\text{S}^{2-}$ or $\text{S}_2\text{O}_3^{2-}$) as reducing agents for generated minorities is proposed. Bi_2S_3 , synthesized via solvent thermal process, has a good crystallinity and exhibits n-type conduction as evidenced from photocurrent-potential characteristics. The flat band potential of Bi_2S_3 ($-0.83\text{V}_{\text{SCE}}$) is pH-insensitive and shifts negatively with increasing S^{2-} concentration by $\sim 53\text{ mV/pS}$. The heterosystem shows a much higher activity than Bi_2S_3 alone where efficient H_2 -photoevolution can be realized with concomitant oxidation of X^{2-} . The optimal value of the mass ratio ($\text{Bi}_2\text{S}_3/\text{TiO}_2$) was equal to unity. In $\text{S}_2\text{O}_3^{2-}$ electrolyte, the photoactivity peaks at pH ~ 13.7 with an evolution rate of $2.9\text{ }\mu\text{mol mg}^{-1}\text{ h}^{-1}$ and decreases gradually to zero near pH 7. The competitive back reduction of end products $\text{S}_4\text{O}_6^{2-}$ and S_2^{2-} slows down the H_2 -evolution. The regression of the photoactivity over time is also due to the decrease of band bending at the interface $\text{TiO}_2/\text{electrolyte}$.

© 2007 Elsevier B.V. All rights reserved.

Keywords: $\text{Bi}_2\text{S}_3/\text{TiO}_2$; Hydrogen; Heterosystem; Photoactivity; Sulfide

1. Introduction

The problem of developing efficient and durable photoelectrochemical (PEC) devices over semiconductors (SC) catalysts for the visible light-to-electrical and/or chemical energy has been actively investigated [1]. Hydrogen photogeneration from inexpensive raw materials like water over optically active SC remains of current interest [2]. Because of the transparency through the visible region of wide band gap SC, most of sun spectrum is subband light and therefore not converted. A way to enhance the photoactivity is to use heterosystems which consist of a wide band gap n-type SC combined with a narrow band gap SC. TiO_2 received a great scientific attention owing to its PEC properties, its wide gap (E_g) makes it an ideal material as window layer. Bi_2S_3 is an important III–VI SC that has been the subject of intensive researches over the last decades owing to its small gap E_g and optoelectronic properties [3]. Only few heterosystems have been investigated probably because of the difficulty of appropriate adjustment of band edges. Bi_2S_3 has a pH-independent double layer through which the energy levels of

the solution are shifted favorably with respect to solid by varying the pH. The electronic bands can be properly matched to the conduction band of TiO_2 ($\text{TiO}_2\text{-CB}$), the latter varies by $\sim 0.59\text{ V}$ per unit change in pH. However, whereas the properties of $\text{Bi}_2\text{S}_3/\text{TiO}_2$ are known in the photodegradation of dyes with some understandings of carriers injection [4], no previous investigations on H_2 -photogeneration have been reported. This heterosystem was studied as bias free H_2 -photocathode using two holes scavengers. The selected materials are inexpensive and this was done in the hope of increasing the efficiency by absorbing more sunlight. This paper deals with the capability of $\text{Bi}_2\text{S}_3/\text{TiO}_2$ for photoassisted water reduction. Hydrogen production by parallel oxidation of inorganic pollutants in powder suspensions is an attractive goal to set up the PEC cell. Sulfur related compounds such as S^{2-} are much easier to oxidize than water and the photodecomposition of H_2S into H_2 and S_2^{2-} was achieved at zero external bias. $\text{S}_2\text{O}_3^{2-}$ is also reported for comparative purpose. Chemical processes are attractive and low-cost techniques for preparing chalcogenides with high specific surface area.

2. Experimental

Ultrafine Bi_2S_3 powder was prepared through solvent thermal process by modifying slightly the method described

* Corresponding author. Tel.: +213 21 24 79 50; fax: +213 21 24 73 11.
E-mail address: mtrari@caramail.com (M. Trari).

elsewhere for CdS synthesis [5]. In our case, $\text{Bi}(\text{NO}_3)_3$ and thiourea with bismuth to sulfur molar ratio ($\text{Bi/S} = 2/3$) were sealed in a 100 cm^3 -Teflon autoclave was filled 80% with absolute ethanol, heated at 150 °C for 12 h and furnace cooled. The introduced mixture contains 5.66 g of $\text{Bi}(\text{NO}_3)_3$, 5 H_2O and 1.33 g of $\text{SC}(\text{NH}_2)_2$. The product was recovered by washing with acetone. It was then treated in diluted acetic acid (6 N) for 30 min to remove preferentially Bi_2O_3 at the external surface and dried at 60 °C overnight. Bi_2S_3 was identified by X-ray diffractometry (XRD) using Ni-filtered $\text{Cu K}\alpha$ radiation. The optical gap was determined thanks to a UV–vis spectrophotometer (Jasco-530) equipped with an integrated sphere.

For PEC properties, Bi_2S_3 was pressed into pellets under 2.25 kbar and heat-treated at 550 °C in evacuated glass tube. For higher temperatures, it decomposes into metal Bi and elemental yellow sulfur. Electrical contact was made with silver paint onto the back side of pellets (compactness $\sim 75\%$) which were then mounted in glass holders using epoxy resin. PEC characterization was done in a nitrogen purged KOH (1 M) using a conventional electrochemical cell. The intensity-potential $J(V)$ characteristics were plotted by a voltalab PGP201 potentiostat and quoted versus a saturated calomel electrode (SCE) via a luggin capillary. The working electrode was brought close to the window to minimize solution light absorption of S^{2-} . A platinum foil (1 cm^2) served as emergency electrode. The apparatus and procedure for the photocatalytic tests were described elsewhere [6]. In brief, the experiments were carried out in a closed gas system equipped with a double walled reactor connected to a water bath whose temperature was maintained at 50 °C by a temperature controller circulator (Julabo III). TiO_2 -P25 (Degussa) was used as received without any further treatment. The powder was suspended in a freshly aqueous X^{2-} electrolyte by magnetic stirring under constant agitation and irradiated by three tungsten lamps (200 W) positioned symmetrically around the reactor. Before starting the tests, the electrolyte was purged of dissolved O_2 by bubbling through with nitrogen for at least 35 min. Evolved hydrogen was identified by gas chromatography and collected in a water manometer because of its low solubility. The pH of solutions was controlled by HNO_3 and NaOH , the chemicals were of analytical quality and the solutions prepared from bi-distilled water.

3. Results and discussion

The XRD pattern of Bi_2S_3 was single phase and the compound crystallizes in an orthorhombic unit cell according to the JCPDS No. 17–320. The cell constants: $a = 1.1650$ nm, $b = 1.1280$ and $c = 0.3980$ nm agree with that of the literature data [7]. Bi_2S_3 has a ribbon like polymeric structure involving S^{2-} bridges in which each Bi and S are surrounded by three ions of opposite kind forming interlocking Bi_2S_3 pyramids.

The reflectance diffuse spectrum presents a well defined absorption edge which is expected for direct transitions. The intercept of $(\alpha h\nu)^2$ with the $h\nu$ axis yields an optical transition of 1.42 eV directly allowed. The low lying VB of $\text{O}^{2-}:2p$ parentage typical of most wide band gap SC oxides is far high to

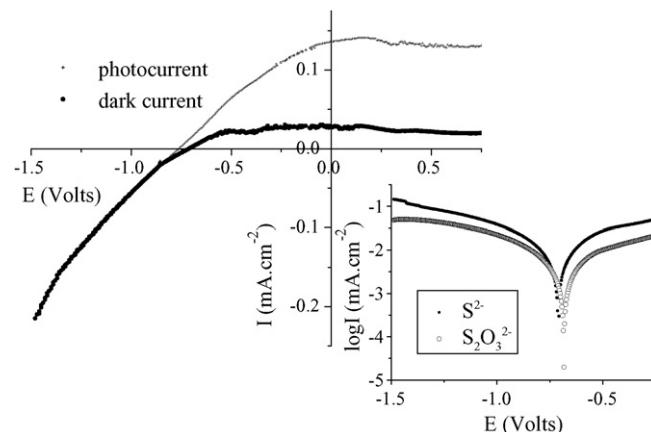


Fig. 1. Linear voltammogram of Bi_2S_3 in 1 M KOH (pH 13.75). Insert: semi-logarithmic plot of X^{2-} over Bi_2S_3 .

make efficient utilization of solar spectrum. By contrast, the electronic bands of Bi_2S_3 are of $\text{S}3p$ character (sulfur is less electronegative than oxygen) and the photoelectrons in CB have a strong ability to reduce H_2O into gaseous H_2 .

The $J(V)$ plots of Bi_2S_3 (Fig. 1) shows that Bi_2S_3 behaves quite irreversibly with large O_2 -overpotential and the polarization is mainly of concentration. The dark current is less than 20 μA in the potential range $-0.8 < V < 1\text{V}$, beyond 1.4 V the current shoots up due to oxygen evolution. The increase of anodic photocurrent J_{ph} under positive polarization is consistent with n-type character. The potential V_{fb} of Bi_2S_3 was taken as that potential below which no photocurrent could be observed and a value of -0.83 V was found. The $J(V)$ curve of TiO_2 (not shown here) plotted under UV irradiation (800 W Halogen lamp) revealed a photo-onset potential assimilated to V_{fb} (-0.55 V), in good agreement with previous results (-0.60 V) [8] (Table 1). Such negative V_{fb} -value should give rise to a large band bending B with a zero (e^-/h^+) pairs recombination. The photocorrosion may be kinetically prevented by using X^{2-} as hole scavenger, the key finding is that S^{2-} enables Bi_2S_3 to be photoelectrochemically stable and shifts cathodically the potential V_{fb} according to the relation: $V_{\text{fb}} = -0.83 - 0.053 \log [\text{S}^{2-}]$.

For practical applications, the fill factor (FF) which characterizes the ideality of the system should be as close as possible to unity with a rectangular shape. It depends on the properties of both SC and redox couple. In our case, the larger short circuit current and open circuit voltage with the non-absorbing $\text{S}_2\text{O}_3^{2-}$ over Bi_2S_3 are attributed to the great

Table 1
The physical properties of Bi_2S_3 and TiO_2

Compound	Color	E_g (eV)	$\rho_{300\text{ K}}$ ($\Omega\text{ cm}$)	$S_{300\text{ K}}$ ($\mu\text{V K}^{-1}$)	ΔE (eV)	V_{fb} (V)	U_f (V)
Bi_2S_3	Dark	1.42	123	−32	0.10 ^b	−0.83	−0.62 ^c
TiO_2	White	3.21 ^a	485 ^d	950	0.07	−0.55	—

^a The band gap energy of TiO_2 was calculated using the wave length at the absorption edge.

^b Measured in the heating direction.

^c Determined in S^{2-} media.

^d Fired in evacuated silica tube.

Table 2
Kinetic parameters of Bi_2S_3 immersed in X^{2-} solutions

Species	Parameters			
	FF	i_0 (mA cm^{-2})	R_p (Ω)	$\partial \log i / \partial V$ (dec. V^{-1})
S^{2-}	0.37	3×10^{-4}	1.34×10^4	0.919
$\text{S}_2\text{O}_3^{2-}$	0.28	2×10^{-5}	2.54×10^4	6.19, 1.22

difference $\{E_{\text{red}} - V_{\text{fb}}\}$. However, the low FF is due to the slow electron transfer where the electrochemical system behaves irreversibly with less favorable $J(V)$ characteristic. Such low FF values are corroborated by semi-logarithmic plots (inset Fig. 1) whose kinetic parameters are given in Table 2. An efficient photosensitive material should have a high exchange current density i_0 , a low electric resistance R_p and a large slope $\partial \log i / \partial V$. The dual slopes in the anodic region with $\text{S}_2\text{O}_3^{2-}$ are attributed to successive oxidations according to reactions (3) and (4) (see below).

The free potential U_f of $n\text{-Bi}_2\text{S}_3$ must be more negative than V_{fb} to eventuate photoreactions and the best case occurs when U_f belongs to the plateau region in the $J_{\text{ph}}(V)$ plot as seems to occur in our case. The photoactivity was greatly dependent on the preparative conditions. Fig. 2 gives the dependence of H_2 -volume obtained after saturation on the concentration C_m (mg catalyst/ml electrolyte). The volume and the rate of H_2 -evolution both increase with C_m giving an optimal value of 1.5 mg/ml above which a decay of the photoactivity is observed. This behavior can be attributed to the fact that at low C_m , enough photons were not absorbed and hence the generated carriers were not sufficient to react with adsorbed water. The photons flux being constant, the number of photogenerated (e^-/h^+) pairs increases with the amount of Bi_2S_3 which goes parallel to the receptive surface and in this way the H_2 -production. By contrast, at high C_m , all photons are absorbed and further increase of photons flux reduces the penetration depth particularly with yellow polysulfides. The light scattering also accounts for the regression of the photoactivity. A constant value is reached and a

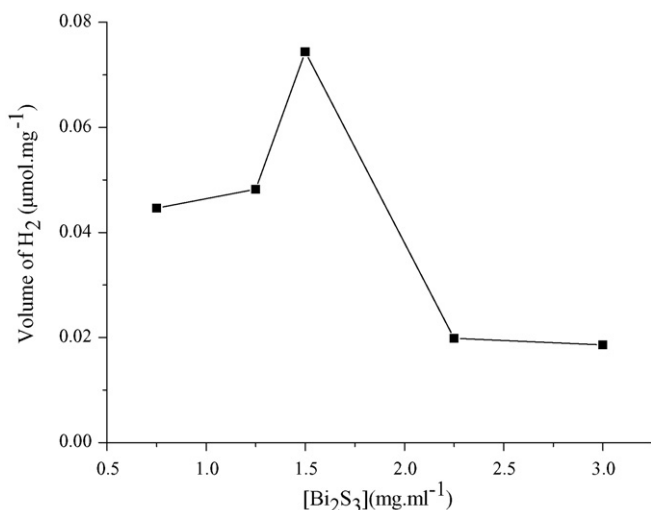


Fig. 2. Effect of the amount of Bi_2S_3 on H_2 -production in S^{2-} solution. Each point was taken after saturation.

particle shadowing is observed beyond 2.25 mg.ml^{-1} where many crystallites are only partially irradiated.

The interfacial rates are governed by the electron transfer through the relative positions of occupied states of redox couple pertained to $\text{H}_2\text{O}/\text{H}_2$ states and $\text{TiO}_2\text{-CB}$. At basic pH, absorption of light promotes electrons into $\text{Bi}_2\text{S}_3\text{-CB}$ with a potential (-0.93 V) sufficient to inject them into $\text{TiO}_2\text{-CB}$ (-0.62 V). This should yield a thermodynamically feasible H_2 production. This fact is attributed to the improvement of the charge carriers separation in comparison with Bi_2S_3 alone. The photoelectrons in $\text{Bi}_2\text{S}_3\text{-CB}$, working as electrons pump, are transferred to $\text{TiO}_2\text{-CB}$ to reduce adsorbed water. In a second step, the photocatalytic tests were performed with various mass concentration C_r ($\text{TiO}_2/\text{Bi}_2\text{S}_3$) keeping constant the mass of Bi_2S_3 and the other parameters. The volume of H_2 at saturation increases with C_r and peaks for C_r equal to unity; the volume decreases when further TiO_2 was added. The photoactivity of Bi_2S_3 appear to act similarly to Cu_2O on TiO_2 improving the kinetic process [4] (Fig. 3).

Decreasing the pH lowers the concentration of free $\text{S}_2\text{O}_3^{2-}$ species and shifts the potential of $\text{H}_2\text{O}/\text{H}_2$ level towards the negative direction but keep the value $\{E(\text{H}_2\text{O}/\text{H}_2) - E(\text{CB}(\text{TiO}_2))\}$ somewhat constant. The potentials vary but differently (0.06 V pH^{-1} for TiO_2 and 0.09 V pH^{-1} for $\text{SO}_3^{2-}/\text{S}_2\text{O}_3^{2-}$). This implies that the interval $\{E(\text{SO}_3^{2-}/\text{S}_2\text{O}_3^{2-}) - E(\text{TiO}_2\text{-CB})\}$ decreases with decreasing pH and the reduced bending B leads to a less efficient charge separation. Moreover, this behavior indicates that the global PEC process is governed kinetically by the anodic oxidations (Fig. 4). The reactions occurring in the anodic and cathodic poles can be summarized as follows:

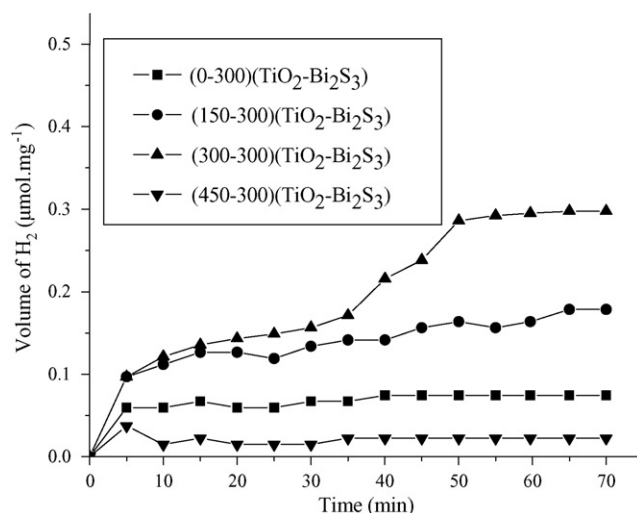


Fig. 3. Time evolution of H_2 -production in S^{2-} solution vs. C_r .

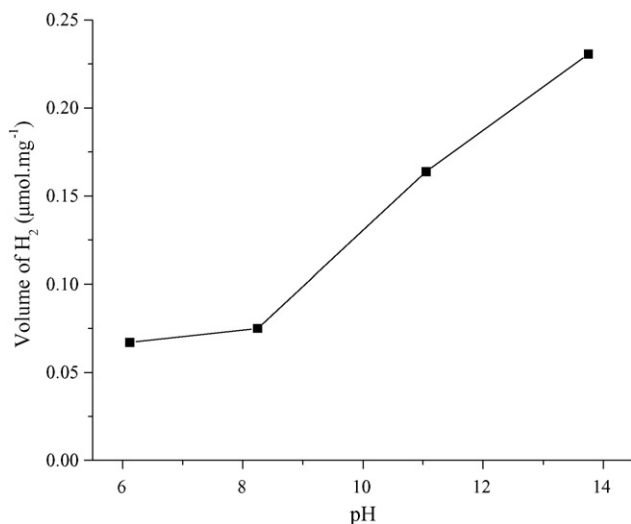


Fig. 4. pH dependence of H₂-evolution at saturation for Bi₂S₃/TiO₂ in S₂O₃²⁻ electrolyte.

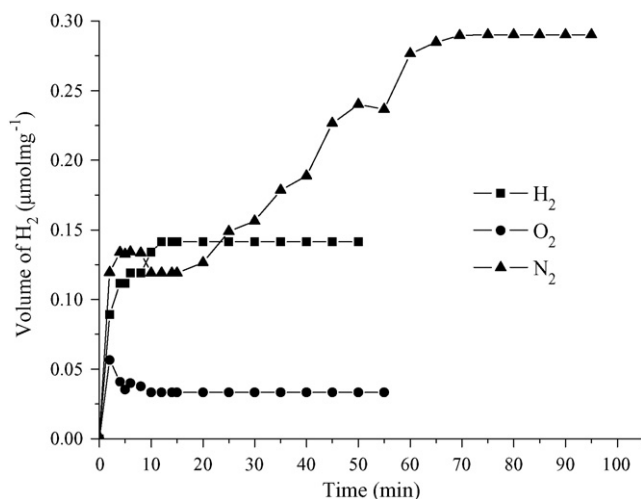


Fig. 5. H₂-evolution after bubbling with: N₂ (▲); H₂ (■); O₂ (●).

The fact that the photoactivity depends on the pH indicates that the reaction (3) dominates over the reaction (4). This results in a decrease of the efficiency by competitive reduction of intermediate product namely SO₃²⁻ that takes place more easily at lower pH [manuscript in preparation]. In the case of S²⁻, the volume of evolved H₂ increases parallel to S₂²⁻ and the color change might be due to the S_n²⁻ formation as reported previously [6].

In a closed vessel, the H₂ photoevolution exhibits a tendency towards saturation. In order to check whether the decrease of the photoactivity was linked to a deactivation effect of the catalyst or to H₂-saturation, the solution was bubbled with nitrogen. H₂ produced during the second irradiation is represented in Fig. 5 (▲). The rate constant, calculated from the slope of the straight line (3.58 mol mg⁻¹ h⁻¹), leads practically to a non deactivation effect of the catalyst. The volume obtained at saturation (~2 cm³) corresponds to a partial

pressure P_{H₂} of 5 × 10⁻³ atm. This implies a potential shift of H₂O/H₂ couple towards the negative direction equal to ~0.15 V (dE = -0.03 log P_{H₂}) and would have the disadvantage to reduce the bending B at the interface TiO₂/electrolyte. The bubbling by hydrogen moves the potential of H₂O/H₂ couple below TiO₂-CB slowing down the H₂ evolution (■, Fig. 5). On the contrary, when O₂ is bubbled in the solution the photoelectrons are lost by forming reactive radical O₂^{-•} with short lifetimes (●, Fig. 5).

4. Conclusion

The improvement of the light-to-chemical energy conversion was achieved through the heterosystem Bi₂S₃/TiO₂. Bi₂S₃ was elaborated by hydrothermal process because the quantity of reaction surface per given catalyst mass is increased. The conductivity of Bi₂S₃ was enhanced with the heat treatment under oxygen free atmosphere for PEC characterization. It is chemically stable in both S²⁻ and S₂O₃²⁻ media. The originality of Bi₂S₃ is that the potential of electronic bands follows a Nernstian slope with respect to sulfide but exhibits a pH-independent flat band potential and can be appropriately positioned to TiO₂-CB. The heterosystem converts photoelectrochemically hydrogen sulfide to hydrogen and disulfide S₂²⁻ in alkaline solution. The enhanced photoactivity was ascribed to photoelectrons transfer from Bi₂S₃-CB to more positive TiO₂-CB resulting in the water reduction with concomitant oxidation of X²⁻ species. The rate of H₂ production increases and peaks for a mass concentration (Bi₂S₃/TiO₂) equal to unity. The best performance was obtained with S²⁻ as evidenced from semi-logarithmic plots. The effect of varying the pH was explored by measuring the rate of H₂ evolution in S₂O₃²⁻ owing to its chemical stability in a large pH range. The photoactivity was nearly restored when the electrolyte was purged of hydrogen by bubbling with N₂.

Acknowledgment

The authors wish to thank Mr. T Gaceb for his technical assistance.

References

- [1] S. Pavasupree, Y. Suzuki, S. Pivsa-Art, S. Yoshikawa, Sci. Technol. Adv. Mater. 6 (2005) 224.
- [2] M. Ni, M.K.H. Leung, D.Y.C. Leung, K. Sumathy, Renew. Sustain. Energy Rev. 11 (2007) 401.
- [3] Y. Bessekhouad, D. Robert, J.-V. Weber, N. Chaoui, J. Photochem. Photobiol. A 167 (2004) 49.
- [4] Y. Bessekhouad, D. Robert, J.V. Weber, Catal. Today 101 (2005) 315.
- [5] S. Yu, Y. Quian, L. Shu, Y. Xie, L. Yang, C. Wang, Mater. Lett. 35 (1998) 116.
- [6] S. Saadi, A. Bouguelia, M. Trari, Solar Energy 80 (2006) 272.
- [7] Nat. Bureau Standards Mono 5 (1967) 13.
- [8] G. Prasad, K.S. Chandra Babu, O.N. Srivastava, Int. J. Hydrogen Energy 539 (1989) 14.